THE EUROPEAN
PHYSICAL JOURNAL C

CrossMark

Top-squark in natural SUSY under current LHC run-2 data

Chengcheng Han[3,a], **Jie Ren**[4,b], **Lei Wu**[1,2,c], **Jin Min Yang**[5,d], **Mengchao Zhang**[6,e]

[1] Department of Physics and Institute of Theoretical Physics, Nanjing Normal University, Nanjing, Jiangsu 210023, China
[2] ARC Centre of Excellence for Particle Physics at the Terascale, School of Physics, The University of Sydney, Sydney, NSW 2006, Australia
[3] Kavli IPMU (WPI), UTIAS, University of Tokyo, Kashiwa 277-8583, Japan
[4] Computer Network Information Center, Chinese Academy of Sciences, Beijing 100190, China
[5] Key Laboratory of Theoretical Physics, Institute of Theoretical Physics, Chinese Academy of Sciences, Beijing 100190, China
[6] Center for Theoretical Physics and Universe, Institute for Basic Science (IBS), Taejon 34051, Korea

Abstract We utilize the recent LHC-13 TeV data to study the lower mass bound on the top-squark (stop) in natural supersymmetry. We recast the LHC sparticle inclusive search of (≥ 1)jets $+ \not{E}_T$ with α_T variable, the direct stop pair search (1-lepton channel and all-hadronic channel) and the mono-jet analyses. We find that these searches are complementary depending on stop and higgsino masses: for a heavy stop the all-hadronic stop pair search provides the strongest bound, for an intermediate stop the inclusive SUSY analysis with α_T variable is most efficient, while for a compressed stop–higgsino scenario the monojet search plays the key role. Finally, the lower mass bound on a stop is: (1) 320 GeV for compressed stop–higgsino scenario (mass splitting less than 20 GeV); (2) 765 (860) GeV for higgsinos lighter than 300 (100) GeV.

1 Introduction

The discovery of the Higgs boson is a great triumph for the Standard Model (SM). However, the SM Higgs mass is quadratically sensitive to the cutoff scale Λ (usually taken as GUT or Planck scale) via radiative corrections because of the lack of symmetry protection. This renders the SM with $m_h \sim 125$ GeV $\ll \Lambda$ rather unnatural. A well-known theory for solving such a naturalness problem is supersymmetry.

Among various supersymmetric models, natural supersymmetry (NSUSY) is a well-motivated framework [1–3], which consists of a small set of sparticles that closely relate to

a e-mail: hancheng@itp.ac.cn
b e-mail: jieren21@live.com
c e-mail: lei.wu1@sydney.edu.au
d e-mail: jmyang@itp.ac.cn
e e-mail: mczhang@itp.ac.cn

the naturalness, such as higgsinos, stop, and gluino. This can be understood by the minimization of the Higgs potential [4],

$$\begin{aligned}
\frac{M_Z^2}{2} &= \frac{(m_{H_d}^2 + \Sigma_d) - (m_{H_u}^2 + \Sigma_u)\tan^2\beta}{\tan^2\beta - 1} - \mu^2 \\
&\simeq -(m_{H_u}^2 + \Sigma_u) - \mu^2,
\end{aligned} \tag{1}$$

where μ is the higgsino mass parameter in the superpotential and contributes to M_Z at tree level, $\tan\beta \equiv v_u/v_d \gg 1$ is assumed in the last approximate equality, $m_{H_d}^2$ and $m_{H_u}^2$ denote the soft SUSY breaking masses of the Higgs fields at weak scale, and Σ_u and Σ_d arise from the radiative corrections to the Higgs potential. Due to the large top Yukawa couplings, Σ_u is dominated by the stop at 1-loop level, while the gluino contributes to Σ_u via the corrections to the stop mass. Other contributions from the first two generation squarks and sleptons to M_Z are negligibly small. Therefore, the requirement of getting the correct value of M_Z without fine-tuning will give upper bounds on the masses of higgsinos, stops, and gluino [5,6]. In the past few years, much work has been devoted to the searches for the stop at the LHC in NSUSY [7–22].

With the recent ~ 15 fb^{-1} dataset at the LHC run-2, the stop and gluino masses are respectively excluded up to ~ 1 TeV [23] and 1.8 TeV [24], while the electroweakinos below 0.4–1 TeV can also be covered for different decay channels [25]. But these limits are obtained in the simplified models [26–28] and sensitively depend on the assumptions of the nature of the lighest supersymmetric partner (LSP), the branching ratios of heavier sparticles and the mass splitting between heavier sparticles and the LSP. Therefore, it is necessary to examine the current LHC run-2 coverage of NSUSY and assess the fine-tuning extent. In this work, we utilize the recent results of the LHC run-2 inclusive sparticle searches and direct stop pair searches to constrain the stop mass in

Springer

NSUSY. We compare their sensitivities and find that they are complementary in probing NSUSY. We will also evaluate the electroweak fine-tuning measure in the allowed parameter space of NSUSY and comment on the prospect for covering the low fine-tuning parameter space of NSUSY at HL-LHC.

2 Constraints on stop in NSUSY

In MSSM, the stop mass matrix in the weak-basis $(\tilde{t}_L, \tilde{t}_R)$ is given by

$$M_{\tilde{t}}^2 = \begin{pmatrix} m_{\tilde{t}_L}^2 & m_t X_t^\dagger \\ m_t X_t & m_{\tilde{t}_R}^2 \end{pmatrix}, \tag{2}$$

with

$$m_{\tilde{t}_L}^2 = m_{\tilde{Q}_{3L}}^2 + m_t^2 + m_Z^2 \left(\frac{1}{2} - \frac{2}{3} \sin^2 \theta_W \right) \cos 2\beta, \tag{3}$$

$$m_{\tilde{t}_R}^2 = m_{\tilde{U}_{3R}}^2 + m_t^2 + \frac{2}{3} m_Z^2 \sin^2 \theta_W \cos 2\beta, \tag{4}$$

$$X_t = A_t - \mu \cot \beta. \tag{5}$$

Here $m_{\tilde{Q}_{3L}}^2$ and $m_{\tilde{U}_{3R}}^2$ are the soft-breaking mass parameters for the third generation left-handed squark doublet $\tilde{Q}_{3L}$ and the right-handed stop $\tilde{U}_{3R}$, respectively. A_t is the stop soft-breaking trilinear parameter. The weak eigenstates $\tilde{t}_{L,R}$ can be rotated to the mass eigenstates $\tilde{t}_{1,2}$ by a unitary transformation,

$$\begin{pmatrix} \tilde{t}_1 \\ \tilde{t}_2 \end{pmatrix} = \begin{pmatrix} \cos \theta_{\tilde{t}} & \sin \theta_{\tilde{t}} \\ -\sin \theta_{\tilde{t}} & \cos \theta_{\tilde{t}} \end{pmatrix} \begin{pmatrix} \tilde{t}_L \\ \tilde{t}_R \end{pmatrix}. \tag{6}$$

After diagonalizing the mass matrix, see Eq. (2), we can have the stop masses $m_{\tilde{t}_{1,2}}$ and the mixing angle $\theta_{\tilde{t}}$ ($-\pi/2 \leq \theta_{\tilde{t}} \leq \pi/2$),

$$m_{\tilde{t}_{1,2}} = \frac{1}{2} \left[m_{\tilde{t}_L}^2 + m_{\tilde{t}_R}^2 \mp \sqrt{\left(m_{\tilde{t}_L}^2 - m_{\tilde{t}_R}^2 \right)^2 + 4 m_t^2 X_t^2} \right], \tag{7}$$

$$\tan 2\theta_{\tilde{t}} = \frac{2 m_t X_t}{m_{\tilde{t}_L}^2 - m_{\tilde{t}_R}^2}. \tag{8}$$

The decays of stop are determined by the interactions between stop and neutralinos/charginos, which are given by

$$\mathcal{L}_{\tilde{t}_1 \bar{b} \tilde{\chi}_i^+} = \tilde{t}_1 \bar{b} (f_L^C P_L + f_R^C P_R) \tilde{\chi}_i^+ + h.c.,$$

$$\mathcal{L}_{\tilde{t}_1 \bar{t} \tilde{\chi}_i^0} = \tilde{t}_1 \bar{t} (f_L^N P_L + f_R^N P_R) \tilde{\chi}_i^0 + h.c., \tag{9}$$

where $P_{L/R} = (1 \mp \gamma_5)/2$ and

$$f_L^N = - \left[\frac{g_2}{\sqrt{2}} N_{i2} + \frac{g_1}{3\sqrt{2}} N_{i1} \right] \cos \theta_{\tilde{t}} - y_t N_{i4} \sin \theta_{\tilde{t}} \tag{10}$$

$$f_R^N = \frac{2\sqrt{2}}{3} g_1 N_{i1}^* \sin \theta_{\tilde{t}} - y_t N_{i4}^* \cos \theta_{\tilde{t}}, \tag{11}$$

$$f_L^C = y_b U_{i2}^* \cos \theta_{\tilde{t}}, \tag{12}$$

$$f_R^C = -g_2 V_{i1} \cos \theta_{\tilde{t}} + y_t V_{i2} \sin \theta_{\tilde{t}}, \tag{13}$$

with $y_t = \sqrt{2} m_t / (v \sin \beta)$ and $y_b = \sqrt{2} m_b / (v \cos \beta)$ being the Yukawa couplings of top and bottom quarks. The mixing matrices of the neutralinos N_{ij} and charginos U_{ij}, V_{ij} are defined in [29]. In NSUSY, $M_{1,2} \gg \mu$, one has $V_{11}, U_{11}, N_{11,12,21,22} \sim 0$, $V_{12} \sim \text{sgn}(\mu)$, $U_{12} \sim 1$ and $N_{13,14,23} = -N_{24} \sim 1/\sqrt{2}$. So, $\tilde{\chi}_1^\pm$ and $\tilde{\chi}_{1,2}^0$ are higgsino-like and nearly degenerate.[1] The left-handed stop will mainly decay to $t \tilde{\chi}_{1,2}^0$ when the phase space is accessible and $\tan \beta$ is small. The couplings of the right-handed stop with $\tilde{\chi}_{1,2}^0$ and $\tilde{\chi}_1^\pm$ are proportional to y_t, and the branching ratios of $\tilde{t}_1 \to t \tilde{\chi}_{1,2}^0$ and $\tilde{t}_1 \to b \tilde{\chi}_1^+$ are about 25 and 50%, respectively.

To address the lower mass limit of the stop in NSUSY, we can focus on a right-handed stop. This is because the left-handed stop is linked with the left-handed sbottom by the $SU(2)$ symmetry. Then the left-handed sbottom decay channel $\tilde{b}_1 \to t \tilde{\chi}_1^-$ can mimics the left-handed stop signals $\tilde{t}_1 \to t \tilde{\chi}_{1,2}^0$ since $\tilde{\chi}_{1,2}^0$ and $\tilde{\chi}_1^+$ are higgsino-like and degenerate in NSUSY. This enhances the LHC limit on a left-handed stop, which is stronger than the limit on a right-handed stop [15,20].

Now we examine the constraints on the NSUSY scenario that consists of a right-handed stop and higgsinos. We scan the parameter space in the ranges

$$100 \text{ GeV} \leq \mu \leq 600 \text{ GeV},$$
$$100 \text{ GeV} \leq m_{\tilde{Q}_{3L}, \tilde{U}_{3R}} \leq 2.5 \text{ TeV},$$
$$1 \text{ TeV} \leq A_t \leq 3 \text{ TeV}, \quad 5 \leq \tan \beta \leq 50. \tag{14}$$

The lower limit on the higgsino mass is motivated by the LEP searches for electroweakinos. We require the stop mixing angle $|\sin \theta_{\tilde{t}}|^2 > 0.5$ to obtain a right-handed stop $\tilde{t}_1$. Since the gluino contributes to the naturalness measure in Eq. (15) at 2-loop level, a low fine-tuning allows the gluino with a mass up to several TeV, which is possibly beyond the reach of LHC. So we assume the gluino mass parameter to be $M_3 = 2$ TeV in our scan. Since the electroweak gauginos, heavy Higgs bosons, the sleptons, the first two generations of squarks and the right-handed sbottom are not strongly related to the naturalness, we decouple their contributions by fixing $M_1 = M_2 = m_A = m_{\tilde{\ell}} = m_{\tilde{q}_{1,2}} = m_{\tilde{D}_R} = 2$ TeV at the weak scale.

In our scan, we impose the following indirect constraints:

- *Higgs mass* We require that the lighter CP-even Higgs boson be the SM-like Higgs boson with a mass in the

---

[1] The detection of such light higgsinos through a monojet (or a monojet-like case) may be challenging at the LHC [30–34].

range of 125 ± 2 GeV, which is calculated by the package FeynHiggs-2.11.2 [35,36].[2]

- *Vacuum stability* We impose the constraint of metastability of the vacuum state by requiring $|A_t| \lesssim 2.67 \sqrt{M_{\tilde{Q}_{3L}}^2 + M_{\tilde{t}_R}^2 + M_A^2 \cos^2 \beta}$ [38], because the large trilinear parameter A_t can potentially lead to a global vacuum where charge and color are broken [38–40].
- *Low-energy observables* We require our samples to satisfy the bound of $B \to X_s \gamma$ at 2σ range, which is implemented by the package of SuperIso v3.3 [41,42].
- *Dark matter detection* We require the thermal relic density of the neutralino dark matter Ωh^2 to be below the 2σ upper limit of 2015 Planck value [43][3] and the LUX WS2014-16 [47]. The results for the spin-independent neutralino–proton scattering cross section σ_p^{SI} is rescaled by a factor of $\Omega h^2 / \Omega_{PL} h^2$. We use the package of MicrOmega v2.4 [48] to calculate Ωh^2 and σ_p^{SI}.

Besides, the LHC run-2 experiments have covered a wide parameter space of the MSSM. We list the relevant LHC experimental analyses for our scenario:

- From ATLAS,
  - **Stop**, 0 lepton + (b)jets + $\not{E}_T$, 13.3 fb^{-1} [49],
  - **Stop**, 1 lepton + (b)jets + $\not{E}_T$, stop, 13.3 fb^{-1} [50],
  - **Stop**, 2 leptons + (b)jets + $\not{E}_T$, stop, 13.3 fb^{-1} [51],
  - **Sbottom**, 2 b-tagged jets + $\not{E}_T$, 3.2 fb^{-1} [52],
  - **Compressed Spectrum**, 1 jet + $\not{E}_T$, 3.2 fb^{-1} [53].

- From CMS,
  - **Inclusive**, 0 lepton + $\geqslant$ 1 jets + $\not{E}_T$ + α_T, 12.9 fb^{-1} [54]
  - **Inclusive**, 0 lepton + $\geqslant$ 1 jets + $\not{E}_T$ + M_{T_2}, 12.9 fb^{-1} [55]
  - **Inclusive**, 0 lepton + $\geqslant$ 1 jets + $\not{E}_T$ + H_T^{miss}, 12.9 fb^{-1} [56]
  - **Stop**, 0 lepton + (b)jets + $\not{E}_T$, 12.9 fb^{-1} [23],
  - **Stop**, 1 lepton + (b)jets + $\not{E}_T$, 12.9 fb^{-1} [57],
  - **Compressed Spectrum**, 1 jet + soft lepton pair + $\not{E}_T$, 12.9 fb^{-1} [58].

---

[2] The prediction of the SM-like Higgs mass depends on the spectrum generators. The differences arise from the choice of the renormalization scheme and the higher order correction calculations. These effects often lead to a few GeV uncertainty for the SM-like Higgs mass in the MSSM [37].

[3] The thermal relic density of the light higgsino-like neutralino dark matter is typically low as a result of the large annihilation rate in the early Universe. One possible way to produce the correct relic density is introducing the mixed axion–higgsino dark matter [44,45]. However, if the naturalness requirement is relaxed, the heavy higgsino-like neutralino with a mass $\sim$1–2 TeV can solely produce the correct relic density in the MSSM [46].

Table 1 The LHC Run-2 analyses used in our study

ATLAS	CMS
1 lepton + (b)jets + $\not{E}_T$ [50]	0 lepton +($\geqslant$1)jets + $\not{E}_T$ + α_T [54]
1 jet + $\not{E}_T$ [53]	0 lepton + (b)jets + $\not{E}_T$ [23]

It should be mentioned that the higgsinos $\tilde{\chi}_1^\pm$ and $\tilde{\chi}_2^0$ have the small mass difference with the LSP $\tilde{\chi}_1^0$ in NSUSY. Then the decay products of $\tilde{\chi}_1^\pm$ and $\tilde{\chi}_2^0$ are too soft to be tagged at the LHC. So, the stop decays can be categorized into two topologies: $2b + \not{E}_T$ and $t\bar{t} + \not{E}_T$. Among the current ATLAS searches for the stop, the all-hadronic final state channel has a better sensitivity than those with leptons in the high stop mass region ($m_{\tilde{t}_1} > 800$ GeV) because of the application of boosted top technique. Similar results are obtained by the CMS Collaboration. With the decrease of the mass splitting $\Delta m_{\tilde{t}_1 - \tilde{\chi}_1^0}$, the sensitivity of the conventional stop searches for the energetic top quark in the final states become poor. In particular, if $\Delta m_{\tilde{t}_1 - \tilde{\chi}_1^0} \ll m_t$, the stop decay will be dominated by the four-body channel $\tilde{t}_1 \to b f' \bar{f} \tilde{\chi}_1^0$ [59,60] or the two-body loop channel $\tilde{t}_1 \to c \tilde{\chi}_1^0$ [61–65]. Then the decay products of the stop are usually very soft so that a high p_T hard jet from the ISR/FSR is needed to tag these compressed stop events, such as the ATLAS monojet analysis listed above. Note that the very recent CMS monojet with the soft lepton pair analysis of the compressed electroweakinos can exclude the wino-like chargino mass $m_{\tilde{\chi}_1^\pm}$ up to 175 GeV for a mass difference of 7.5 GeV with respect to the LSP. However, this limit is not applicable to our scenario because the cross section of the higgsino pair production is 1/4 of the wino pair. On the other hand, both ATLAS and CMS experiments have performed the inclusive SUSY searches for final states with (generally untagged) jets and a large amount of $\not{E}_T$, which can also be used to derive limits on the parameter space in various simplified models. In our study, we reinterpret the recent CMS analysis of $0-\text{lepton} + (\geqslant 1)\text{jets} + \not{E}_T$. This strategy is built around the use of the kinematic variable α_T, which is constructed from jet-based quantities to provide strong discriminating power between sources of genuine and misreconstructed $\vec{p}_T^{\text{miss}}$. Such a variable can highly suppress multijet background, and is suitable for early searches at 13 TeV LHC. Based on the above considerations, we use four LHC experimental analyses to constrain the parameter space of NSUSY, which are listed in Table 1.

In our Monte Carlo simulations, we use MadGraph5_aMC@NLO [66] to generate the parton level signal events, which are showered and hadronized by the package PYTHIA [67]. The detector simulation effects are implemented with the package Delphes [68]. The jets are clustered with the anti-k_t algorithm [69] by the package FastJet [70]. The cross section of the stop pair production at 13 TeV
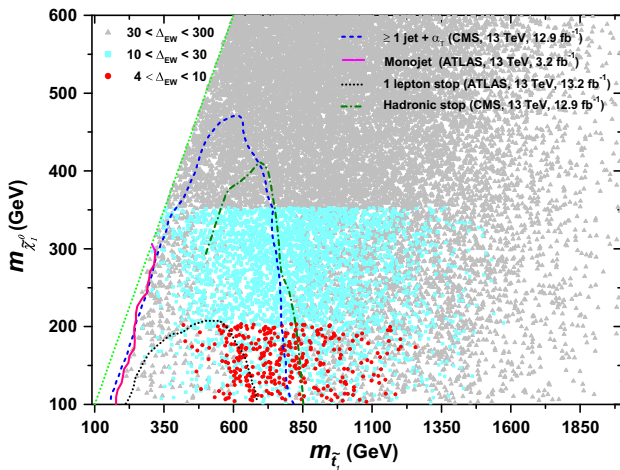
Fig. 1 *Scatter plots* on the plane of $m_{\tilde{t}_1}$ versus $m_{\tilde{\chi}_1^0}$. All samples satisfy the constraints of the Higgs mass, vacuum stability, $B \to X_s \gamma$, and dark matter detections. The exclusion limits of the LHC SUSY searches in Table 1 are recast. The *triangles* (*gray*), *squares* (*cyan*) and *bullets* (*red*) represent the samples that have the electroweak fine-tuning $\Delta_{EW} < 10$, $10 < \Delta_{EW} < 30$ and $30 < \Delta_{EW} < 300$, respectively

LHC are calculated by NLL-fast package [71–75] with the CTEQ6.6M PDFs [76]. We impose the ATLAS monojet constraint with MadAnalysis 5-1.1.12 [77–79]. The ATLAS 1-lepton stop and the CMS 0-lepton stop analyses are implemented within the CheckMATE framework [80,81]. But as mentioned above, we only focus on the heavy stop mass range ($m_{\tilde{t}_1} > 500$ GeV) for the CMS 0-lepton analyses because of the improved sensitivity by application of the top tagging technique. Besides, the higgsinos $\tilde{\chi}_1^\pm$ and $\tilde{\chi}_{1,2}^0$ are nearly degenerate in NSUSY. The stop decay $\tilde{t} \to b \tilde{\chi}_1^+$ gives the same topology as the sbottom decay $\tilde{b} \to b \tilde{\chi}_1^0$. So we can determine the exclusion limit on the stop by using the cross section upper limit of the sbottom pair production reported from the CMS inclusive search with α_T.

In Fig. 1, we project the samples allowed by the Higgs mass, vacuum stability, $B \to X_s \gamma$ and dark matter detections on the plane of $m_{\tilde{t}_1}$ versus $m_{\tilde{\chi}_1^0}$. To quantitatively evaluate the naturalness, we use the electroweak fine-tuning measure Δ_{EW}[4] [82]; we have

$$\Delta_{EW} \equiv max_i |C_i| / (M_Z^2/2), \tag{15}$$

where $C_\mu = -\mu^2$, $C_{H_u} = -m_{H_u}^2 \tan^2 \beta / (\tan^2 \beta - 1)$, $C_{H_d} = m_{H_d}^2 / (\tan^2 \beta - 1)$, $C_{\Sigma_u(i)} = -\Sigma_u(i)(\tan^2 \beta)/(\tan^\beta - 1)$, and $C_{\Sigma_d(i)} = \Sigma_d(i)/(\tan^\beta - 1)$ with i labeling the various loop contributions by Σ_u and Σ_d. The one-loop stop contributions $\Sigma_u(\tilde{t}_{1,2})$ are given by [83].

---

[4] The Barbieri and Guidice (BG) measure in Ref. [5] is applicable to a theory with several independent effective theory parameters. But for a more fundamental theory, the BG measure often leads to an overestimate of fine-tuning [82].

$$\Sigma_u^u(\tilde{t}_{1,2}) = \frac{3}{16\pi^2} F(m_{\tilde{t}_{1,2}}^2)$$
$$\times \left[y_t^2 - g_Z^2 \mp \frac{f_t^2 A_t^2 - 8g_Z^2(\frac{1}{4} - \frac{2}{3} x_W)\Delta_t}{m_{\tilde{t}_2}^2 - m_{\tilde{t}_1}^2} \right] \tag{16}$$

where the form factor $F(m^2) = m^2 \left(\log \frac{m^2}{Q^2} - 1 \right)$ with the optimized scale $Q^2 = m_{\tilde{t}_1} m_{\tilde{t}_2}$, y_t is the top quark Yukawa coupling and $\Delta_t = (m_{\tilde{t}_L}^2 - m_{\tilde{t}_R}^2)/2 + M_Z^2 \cos 2\beta(\frac{1}{4} - \frac{2}{3} x_W)$, $x_W \equiv \sin^2 \theta_W$. In this figure the triangles, squares, and bullets represent the samples that have the electroweak fine-tuning $4 < \Delta_{EW} < 10$, $10 < \Delta_{EW} < 30$ and $30 < \Delta_{EW} < 300$, respectively. In our parameter space, the low fine-tuning $4 < \Delta_{EW} < 10$ requires the higgsino mass $\mu \lesssim 200$ GeV and the stop mass 0.4 TeV $\lesssim m_{\tilde{t}_1} \lesssim 1.3$ TeV. It can be seen that 70% of such a parameter space can be covered by the current LHC Run-2 SUSY searches. A lighter stop mass ($m_{\tilde{t}_1} \lesssim 0.4$ TeV) requires a large trilinear parameter A_t to satisfy the Higgs mass constraint, which leads to a large value of Δ_{EW}.

Besides, from Fig. 1 it can be seen that the ATLAS monojet search produces a strong exclusion limit in the low stop mass region, which excludes the stop mass up to 320 GeV for $m_{\tilde{\chi}_1^0} = 300$ GeV. This is because when the stop mass is close to the LSP mass, the b-jets from the stop decay $\tilde{t}_1 \to b\tilde{\chi}_1^+/bf\bar{f}'\tilde{\chi}_{1,2}^0$ or c-jets from $\tilde{t}_1 \to c\tilde{\chi}_{1,2}^0$ are too soft to be identified. Then the monojet search is very sensitive in the low stop region.

In the moderate or heavy stop region, the stop dominantly decays to $b\tilde{\chi}_1^+$ and $t\tilde{\chi}_{1,2}^0$, which produce $2b + E_T^{miss}$ and $t\bar{t} + E_T^{miss}$ signatures, respectively. The CMS inclusive search with α_T shows a better sensitivity than the 0/1-lepton stop searches in most of parameter space. But we also note that the exclusion limit of the CMS 0-lepton stop search is slightly stronger than the CMS inclusive search because of the application of top tagging technique in ATLAS analysis. Finally, we conclude that the stop mass can be excluded up to 765 (850) GeV for $m_{\tilde{\chi}_1^0} < 300$ ($m_{\tilde{\chi}_1^0} = 100$) GeV by the current LHC Run-2 experiments. Such limits are much stronger than the LHC run-1 limits on NSUSY, which excluded a stop below 600 GeV [15,16,18,20].

It should be mention that when the stop and LSP mass splitting $\Delta m_{\tilde{t}_1 - \tilde{\chi}_1^0} \simeq m_t$, the kinematics of the top quarks from stop decay are similar to those in the top pair production so that the above LHC searches for stop pair have the poor sensitivity. With the help of an additional high momentum jet recoiling against stop pair system, one can utilize the observable $R_M \equiv E_T/p_T(j_{ISR})$ to extend the reach of stop to about 800 GeV at 13 TeV LHC with $\mathcal{L} = 3000$ fb^{-1} [84]. Besides, the VBF production of the stop pair was also proposed to detect such a compressed stop region, which can cover the stop mass to about 300 GeV because of the

large systematical uncertainty [85]. In NSUSY, when both decay channels $\tilde{t}_1 \to t\tilde{\chi}_1^0$ and $\tilde{t}_1 \to b\tilde{\chi}_1^+$ are allowed, search for the asymmetric final states $\tilde{t}(\to t\tilde{\chi}_1^0)\tilde{t}^\dagger(\to b\tilde{\chi}_1^-)$ can provide a complementary way to probing stop at the LHC. With the variable topness to suppress $t\bar{t}$ background, such an asymmetric stop search has a comparable sensitivity with the symmetric stop searches at the HL-LHC [86]. Therefore, together with conventional LHC search strategies, we can expect that the future high luminosity LHC is able to probe the stop and higgsino mass up to 1.5 and 0.6 TeV, respectively [87]. At that time, most of the NSUSY parameter space with $\Delta_{\mathrm{EW}} < 30$ can be covered [87,88].

3 Conclusions

In this paper, we examined the lower mass limit of the stop in natural supersymmetry (NSUSY) by using the recent LHC-13 TeV data. We recast the LHC SUSY inclusive search for ($\geq$1)jets $+ \not{E}_T$ events with α_T variable, the direct stop pair searches (1-lepton channel and all-hadronic channel) and the monojet analyses. We found that the inclusive SUSY analysis with α_T is complementary to the direct stop pair analyses in probing NSUSY. The current LHC data can exclude the stop up to 765 (860) GeV for $m_{\tilde{\chi}_1^0} < 300$ ($m_{\tilde{\chi}_1^0} = 100$) GeV. While in the compressed region ($\Delta m_{\tilde{t}_1 - \tilde{\chi}_1^0} \simeq 20$ GeV), the stop mass can be still light as 320 GeV. About 70% of the NSUSY parameter space with $\Delta_{\mathrm{EW}} < 10$ can be covered by the current LHC Run-2 data. The future HL-LHC is expected to push the lower mass limits of the stop and higgsino up to 1.5 and 0.6 TeV, respectively, and cover most NSUSY parameter space with $\Delta_{\mathrm{EW}} < 30$.

References

1. L.J. Hall, D. Pinner, J.T. Ruderman, JHEP **1204**, 131 (2012)
2. M. Papucci, J.T. Ruderman, A. Weiler, JHEP **1209**, 035 (2012)
3. C. Brust, A. Katz, S. Lawrence, R. Sundrum, JHEP **1203**, 103 (2012)
4. R. Arnowitt, P. Nath, Phys. Rev. D **46**, 3981 (1992)
5. R. Barbieri, G.F. Giudice, Nucl. Phys. B **306**, 63 (1988)
6. H. Baer, V. Barger, M. Savoy, Phys. Rev. D **93**(3), 035016 (2016)
7. H. Baer, V. Barger, P. Huang, A. Mustafayev, X. Tata, Phys. Rev. Lett. **109**, 161802 (2012)
8. H. Abe, T. Kobayashi, Y. Omura, Phys. Rev. D **76**, 015002 (2007). doi:10.1103/PhysRevD.76.015002. arXiv:hep-ph/0703044 [HEP-PH]
9. H. Baer, V. Barger, D. Mickelson, M. Padeffke-Kirkland, Phys. Rev. D **89**(11), 115019 (2014)
10. H. Baer, V. Barger, P. Huang, D. Mickelson, A. Mustafayev, W. Sreethawong, X. Tata, JHEP **1312**, 013 (2013). (Erratum: [JHEP **1506**, 053 (2015)])
11. Z. Kang, J. Li, T. Li, JHEP **1211**, 024 (2012)
12. H. Baer, V. Barger, P. Huang, X. Tata, JHEP **1205**, 109 (2012)
13. J. Cao, C. Han, L. Wu, J.M. Yang, Y. Zhang, JHEP **1211**, 039 (2012)
14. G.D. Kribs, A. Martin, A. Menon, Phys. Rev. D **88**, 035025 (2013)
15. C. Han, K. Hikasa, L. Wu, J.M. Yang, Y. Zhang, JHEP **1310**, 216 (2013)
16. K. Kowalska, E.M. Sessolo, Phys. Rev. D **88**(7), 075001 (2013)
17. G. Belanger, D. Ghosh, R. Godbole, S. Kulkarni, JHEP **1509**, 214 (2015)
18. A. Kobakhidze, N. Liu, L. Wu, J.M. Yang, M. Zhang, Phys. Lett. B **755**, 76 (2016)
19. K. Hikasa, J. Li, L. Wu, J.M. Yang, Phys. Rev. D **93**(3), 035003 (2016)
20. M. Drees, J.S. Kim, Phys. Rev. D **93**(9), 095005 (2016)
21. D. Goncalves, K. Sakurai, M. Takeuchi. arXiv:1604.03938 [hep-ph]
22. G.H. Duan, K.I. Hikasa, L. Wu, J.M. Yang, M. Zhang. arXiv:1611.05211 [hep-ph]
23. The CMS collaboration, CMS-PAS-SUS-16-029
24. The ATLAS collaboration, ATLAS-CONF-2015-067
25. The CMS collaboration, CMS-PAS-SUS-16-024
26. J. Fan, R. Krall, D. Pinner, M. Reece, J.T. Ruderman, JHEP **1607**, 016 (2016)
27. K. Kowalska. arXiv:1608.02489 [hep-ph]
28. A. Barr, J. Liu. arXiv:1605.09502 [hep-ph]
29. J.F. Gunion, H.E. Haber, Nucl. Phys. B **272**, 1 (1986)
30. G.F. Giudice, A. Pomarol, Phys. Lett. B **372**, 253 (1996)
31. H. Baer, V. Barger, P. Huang, JHEP **1111**, 031 (2011)
32. C. Han, A. Kobakhidze, N. Liu, A. Saavedra, L. Wu, J.M. Yang, JHEP **1402**, 049 (2014)
33. Z. Han, G.D. Kribs, A. Martin, A. Menon, Phys. Rev. D **89**, 075007 (2014)
34. C. Han, D. Kim, S. Munir, M. Park, JHEP **1504**, 132 (2015)
35. S. Heinemeyer, W. Hollik, G. Weiglein, Comput. Phys. Commun. **124**, 76 (2000)
36. S. Heinemeyer, W. Hollik, G. Weiglein, Eur. Phys. J. C **9**, 343 (1999)
37. J.P. Vega, G. Villadoro, JHEP **1507**, 159 (2015). doi:10.1007/JHEP07(2015)159
38. D. Chowdhury, R.M. Godbole, K.A. Mohan, S.K. Vempati, JHEP **1402**, 110 (2014)
39. J.E. Camargo-Molina, B. Garbrecht, B. O'Leary, W. Porod, F. Staub, Phys. Lett. B **737**, 156 (2014)
40. U. Chattopadhyay, A. Dey, JHEP **1411**, 161 (2014)
41. F. Mahmoudi, Comput. Phys. Commun. **180**, 1579 (2009)
42. F. Mahmoudi, Comput. Phys. Commun. **178**, 745 (2008)
43. P.A.R. Ade et al. [Planck Collaboration]. arXiv:1303.5076 [astro-ph.CO]
44. H. Baer, A. Lessa, S. Rajagopalan, W. Sreethawong, JCAP **1106**, 031 (2011)
45. H. Baer, A. Lessa, W. Sreethawong, JCAP **1201**, 036 (2012)

46. N. Arkani-Hamed, A. Delgado, G.F. Giudice, Nucl. Phys. B **741**, 108 (2006)
47. D.S. Akerib et al. arXiv:1608.07648 [astro-ph.CO]
48. G. Belanger et al., Comput. Phys. Commun. **182**, 842 (2011)
49. The ATLAS collaboration, ATLAS-CONF-2016-077
50. The ATLAS collaboration, ATLAS-CONF-2016-050
51. The ATLAS collaboration, ATLAS-CONF-2016-076
52. M. Aaboud et al. [ATLAS Collaboration]. arXiv:1606.08772 [hep-ex]
53. M. Aaboud et al. [ATLAS Collaboration], Phys. Rev. D **94**(3), 032005 (2016)
54. The CMS collaboration, CMS-PAS-SUS-16-016
55. The CMS collaboration, CMS-PAS-SUS-16-015
56. The CMS collaboration, CMS-PAS-SUS-16-014
57. The CMS collaboration, CMS-PAS-SUS-16-028
58. The CMS collaboration, CMS-PAS-SUS-16-025
59. A. Djouadi, Y. Mambrini, Phys. Rev. D **63**, 115005 (2001)
60. C. Boehm, A. Djouadi, Y. Mambrini, Phys. Rev. D **61**, 095006 (2000)
61. K. Hikasa, M. Kobayashi, Phys. Rev. D **36**, 724 (1987)
62. T. Han, K. Hikasa, J.M. Yang, X. Zhang, Phys. Rev. D **70**, 055001 (2004)
63. M. Muhlleitner, E. Popenda, JHEP **1104**, 095 (2011)
64. R. Grober, M. Muhlleitner, E. Popenda, A. Wlotzka, Phys. Lett. B **747**, 144 (2015)
65. J. Aebischer, A. Crivellin, C. Greub, Phys. Rev. D **91**(3), 035010 (2015). arXiv:1410.8459 [hep-ph]
66. J. Alwall et al., JHEP **1407**, 079 (2014)
67. T. Sjostrand, S. Mrenna, P.Z. Skands, JHEP **0605**, 026 (2006)
68. J. de Favereau et al. [DELPHES 3 Collaboration], JHEP **1402**, 057 (2014)
69. M. Cacciari, G.P. Salam, G. Soyez, JHEP **0804**, 063 (2008)
70. M. Cacciari, G.P. Salam, G. Soyez, Eur. Phys. J. C **72**, 1896 (2012)
71. W. Beenakker et al., Int. J. Mod. Phys. A **26**, 2637 (2011)
72. A. Kulesza, L. Motyka, Phys. Rev. D **80**, 095004 (2009)
73. W. Beenakker et al., JHEP **0912**, 041 (2009)
74. A. Kulesza, L. Motyka, Phys. Rev. Lett. **102**, 111802 (2009)
75. W. Beenakker, R. Hopker, M. Spira, P.M. Zerwas, Nucl. Phys. B **492**, 51 (1997)
76. D. Stump et al., JHEP **0310**, 046 (2003). arXiv:hep-ph/0303013
77. E. Conte, B. Dumont, B. Fuks, C. Wymant, Eur. Phys. J. C **74**(10), 3103 (2014)
78. B. Dumont et al., Eur. Phys. J. C **75**(2), 56 (2015)
79. D. Sengupta. doi:10.7484/INSPIREHEP.DATA.GTH3.RN26
80. M. Drees et al., Comput. Phys. Commun. **187**, 227 (2014)
81. J.S. Kim et al. arXiv:1503.01123 [hep-ph]
82. H. Baer, V. Barger, D. Mickelson, Phys. Rev. D **88**(9), 095013 (2013)
83. H. Baer, V. Barger, P. Huang, D. Mickelson, A. Mustafayev, X. Tata, Phys. Rev. D **87**(11), 115028 (2013)
84. H. An, L.T. Wang, Phys. Rev. Lett. **115**, 181602 (2015). doi:10.1103/PhysRevLett.115.181602. arXiv:1506.00653 [hep-ph]
85. B. Dutta et al., Phys. Rev. D **90**(9), 095022 (2014). doi:10.1103/PhysRevD.90.095022. arXiv:1312.1348 [hep-ph]
86. M. L. Graesser, J. Shelton, Phys. Rev. Lett. **111**(12), 121802 (2013). doi:10.1103/PhysRevLett.111.121802. arXiv:1212.4495 [hep-ph]
87. J.S. Kim, K. Rolbiecki, R. Ruiz, J. Tattersall, T. Weber. arXiv:1606.06738 [hep-ph]
88. H. Baer, V. Barger, M. Savoy, X. Tata, Phys. Rev. D **94**(3), 035025 (2016)